Environmental Health Perspectives
Vol. 88, pp. 209–218, 1990

Airflow, Gas Deposition, and Lesion Distribution in the Nasal Passages

by Kevin T. Morgan* and Thomas M. Monticello*

The nasal passages of laboratory animals and man are complex, and lesions induced in the delicate nasal lining by inhaled air pollutants vary considerably in location and nature. The distribution of nasal lesions is generally a consequence of regional deposition of the inhaled material, local tissue susceptibility, or a combination of these factors. Nasal uptake and regional deposition are influenced by numerous factors including the physical and chemical properties of the inhaled material, such as water solubility and reactivity; airborne concentration and length of exposure; the presence of other air contaminants such as particulate matter; nasal metabolism, and blood and mucus flow. For certain highly water-soluble or reactive gases, nasal airflow patterns play a major role in determining lesion distribution. Studies of nasal airflow in rats and monkeys, using casting and molding techniques combined with a water-dye model, indicate that nasal airflow patterns are responsible for characteristic differences in the distribution of nasal lesions induced by formaldehyde in these species. Local tissue susceptibility is also a complex issue that may be a consequence of many factors, including physiologic and metabolic characteristics of the diverse cell populations that comprise each of the major epithelial types lining the airways. Identification of the principal factors that influence the distribution and nature of nasal lesions is important when attempting the difficult process of determining potential human risks using data derived from laboratory animals. Toxicologic pathologists can contribute to this process by carefully identifying the site and nature of nasal lesions induced by inhaled materials.

Introduction

Rats and mice are used extensively for inhalation toxicology studies designed to assess the risks or understand mechanisms of diseases in humans. Until recently the nose received much less attention than the lower respiratory tract in inhalation toxicology studies. It was not until 1981 (*1*) that a detailed procedure for histologic preparation of rodent nasal passages for inhalation toxicology studies was published. Since that time many inhalation studies have been performed, revealing many features of the rodent nasal passages. Simultaneously, there has been fairly extensive research on the physiology, biochemistry, and morphology of the nose of rodents and other laboratory animals. Studies of the nose have also been increased by recent interest in the use of this organ as a route for the delivery of drugs and other pharmaceuticals. The toxicologic pathologist can play an important role in this research process by adequately determining and reporting the nature and location of lesions in the nasal passages of animals in toxicology studies (*2*).

*Chemical Industry Institute of Toxicology, P.O. Box 12137, Research Triangle Park, NC 27709.

Address reprints to K. T. Morgan, CIIT, P.O. Box 12137, Research Triangle Park, NC 27709.

This article will briefly review literature on site specificity of nasal lesions induced in laboratory animals by exposure to inhaled gases (or vapors). Subsequently, factors that account for the location of nasal lesions will be discussed with special reference to nasal airflow and effects of formaldehyde. The role of tissue susceptibility will also be addressed briefly, using the nasal toxicity of methyl bromide as an example.

Site Specificity of Nasal Lesions

It is important to note that both nonneoplastic and neoplastic responses in the nasal passages generally occur in specific locations. This has been found to be true not only for inhaled materials, but also for substances delivered by parenteral injection, in food, or drinking water. Our interest in the site specificity of nasal lesions was a consequence of the Chemical Industry Institute of Toxicology (CIIT) research program on formaldehyde toxicity and carcinogenesis. A chronic inhalation study resulted in the finding that 15 ppm formaldehyde is carcinogenic in rats (*3*). Reexamination of the microscope slides from this study revealed clear site specificity for formaldehyde-induced squamous cell carcinomas (*4*). This finding increased our interest in site specificity of lesions and led to the mapping of lesions induced by formaldehyde in rhesus monkeys (*5*) and other gases in rodents (*2*). Much of our experience of mapping of toxic

responses in the nose is limited to gaseous irritants, where the literature on other materials rarely describes the precise location of nasal lesions.

Table 1 provides a list of examples of site-specific nasal lesions, selected to display the variety of sites affected (*6–22*). Figure 1 indicates examples of sites of nasal lesions found in toxicology studies using rats.

For irritant gases, a number of points became evident from our studies. The squamous epithelium of the nasal vestibule is fairly resistant to toxic gases. However, when lesions are present, they most frequently occur on the margins of the anterior extensions of the naso- and maxilloturbinates (the alar folds or the atrioturbinates). In rats exposed to sufficiently high concentrations of highly water-soluble gaseous irritants such as formaldehyde, the respiratory mucosa is frequently affected in multiple locations. These locations include much of the epithelium lining the lateral meatus, especially on the lateral scroll and lateral ridge of the nasoturbinate and the lateral wall adjacent to these structures. Other common sites of respiratory epithelial lesions are those regions bounding the anterior portion of the middle meatus, including the ventral margin of the nasoturbinate, the dorsal margin of the maxilloturbinate, and the septum adjacent to those margins. The most common site of olfactory epithelial lesions is the narrow extension of this epithelium into the anterior half of the dorsal meatus, a region that is very prone to histologic artifacts and is readily overlooked during routine examination of nasal sections. Thus, awareness of site specificity of nasal lesions is important for histotechnologists and pathologists working in the field of toxicology. Such awareness will result in optimal selection and preparation of nasal sections and identification of treatment-induced lesions.

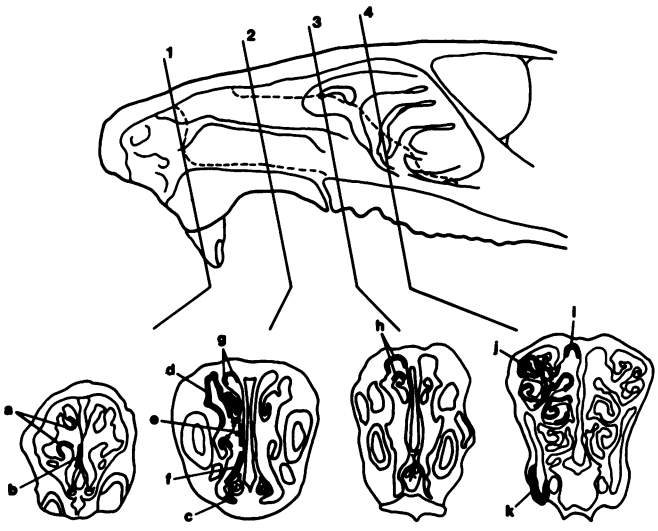

FIGURE 1. Diagram of nasal passages of the rat opened along the midline with the septum removed to reveal the turbinates (upper diagram). Lines numbered 1–4 indicate section levels used routinely in this laboratory, which are shown in lower portion of the figure. Important sites to look for nasal lesions are indicated on the cross sections (refer to Table 1 for details of lesions). (a) Tips of atrioturbinates, (b) septum in nasal vestibule, (c) squamous epithelium in ventral meatus, (d) lining of lateral meatus, (e) margins of middle meatus: ventral margin of nasotrubinate, dorsal margin of maxilloturbinate, and adjacent septum, (f) ventral septum, (g, h, i) olfactory epithelium in dorsal meatus, (j) olfactory mucosa on ethmoid scrolls, and (k) Steno's gland.

Factors That Influence Nasal Lesion Distribution

Two major factors influence the distribution of lesions in the respiratory tract by chemical gases or vapors: regional deposition of the chemical in the nose and local tissue susceptibility. Nasal lesions induced by formaldehyde and methyl bromide (Fig. 2) provide useful examples of each of mechanism. Formaldehyde-induced lesions are largely attributable to regional deposition as a result of airflow patterns, while lesions induced in the olfactory epithelium by methyl bromide are probably a consequence of regional tissue susceptibility. These issues are discussed below with special reference to studies of nasal airflow.

Deposition

Numerous studies have been carried out in several different species on the deposition (uptake, absorption, retention) of airborne chemicals by the nose. These studies can be divided into two main types: uptake studies that investigate the ability of the nose or the upper airways to remove materials from inspired air and thus provide protection to the lower airways; and regional deposition studies that are designed to determine which areas of the nose or upper airways receive the highest dose of the deposited material. For information on general principles of gas and vapor uptake by the

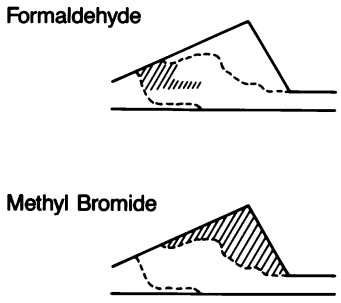

FIGURE 2. Diagrammatic representation of the nasal passages of the rat showing location of three major epithelial types: anterior, squamous; middle, respiratory; posterior, olfactory. Cross-hatching indicates location of lesions induced by formaldehyde and methyl bromide.

Table 1. Selected examples of site-specific responses to xenobiotics in the nose.

Nature of lesion	Principal site	Chemical	Species	Route of administration	Reference
Squamous epithelial region					
Necrosis of squamous epithelium	Ventral meatus	Hydrogen chloride	Mouse	Inhalation	(*2*)
Ulceration	Margins of anterior extensions of turbinates and adjacent lateral wall	Dimethylamine	Rat	Inhalation	(*6*)
Transitional epithelial region					
Necrosis, hyperplasia, inflammation	Transitional zone	Ozone	Monkey	Inhalation	(*7*)
Respiratory epithelial region					
Edema, necrosis, desquamation	Nasomaxillary turbinates	Sulfur dioxide	Mouse	Inhalation	(*8*)
Epithelial degeneration, erosion, and inflammation	Margins of naso-and maxilloturbinates	Chlorine	Rat and mouse	Inhalation	(*9*)
Deciliation, hyperplasia, loss of goblet cells	Margins of middle turbinate, adjacent lateral wall and septum	Chlorine	Monkey	Inhalation	(*10*)
Deciliation, erosion, inflammation, squamous metaplasia	Respiratory epithelium adjacent to the nasal vestibule	Epichlorohydrin, sulfur dioxide, chloropicrin, ammonia, dimethylamine, formaldehyde, hydrogen chloride, toluene diisocyanate	Mouse	Inhalation	(*11*)
Erosions	Dorsal margin of maxilloturbinate, lateral scroll and lateral ridge of nasoturbinate, and adjacent lateral wall	Dimethylamine	Rat	Inhalation	(*6*)
Epithelial vacuolation	Anterior third of nose	Dimethylamine	Rat	Inhalation	(*6*)
Squamous metaplasia	Naso- and maxillo-turbinates and septum	1,2-Dibromo-3-dichloropropane or 1,2-dibromoethane	Rat and mouse	Inhalation	(*12*)
Squamous metaplasia	Lateral and middle meati	Formaldehyde	Rat	Inhalation	(*13*)
Squamous metaplasia	Nasal antrum and margins of middle turbinate	Formaldehyde	Monkey	Inhalation	(*5*)
Polypoid adenomas	Free margins of naso- and maxilloturbinates and adjacent lateral wall	Formaldehyde[a]	Rat		(*4*)
Squamous cell carcinoma	Lateral meatus and ventral septum	Formaldehyde	Rat	Inhalation	(*4*)
Squamous cell carcinoma	Anterior nose	Hexamethyl phosphoramide	Rat	Inhalation	(*14*)
Squamous cell carcinoma	Dorsal and lateral meati	1,4-Dioxane	Rat	Drinking water	(*15*)
Squamous metaplasia, polyp or papilloma, squamous cell carcinoma	Anterior nose: naso-maxillary turbinates, septum, lateral wall	Alkylating agents	Rat	Inhalation	(*16*)
Nasal carcinomas	Anterior curvature of middle turbinate	Nickel dust	Man	Inhalation	(*17*)
Olfactory epithelial region					
Focal atrophy, necrosis of olfactory epithelium	Olfactory epithelium	1,2-Dibromo-3-chloropropane or 1,2-dibromoethane	Rat and mouse	Inhalation	(*12*)
Epithelial degeneration	Dorsal meatus	Chlorine, sulfur dioxide, acrolein, dimethylamine, toluene diisocyanate	Mouse	Inhalation	(*11*)
Epithelial degeneration	Entire olfactory region	Methyl bromide	Rat	Inhalation	(*18*)
Epithelial degeneration	Olfactory mucosa	3-Methylfuran	Rat	Inhalation	(*19*)
Epithelial degeneration	Dorsal meatus	Chlorine, sulfur dioxide, dimethylamine	Rat	Inhalation	(*11*)
Necrosis of Bowman's glands	Olfactory mucosa	NNK[b]	Rat	IP or SC[b]	(*20*)
Neuroepithelioma	Olfactory epithelium	Many nitrosamines	Hamster	Multiple	(*21*)
Esthesioneuroepithelioma	Olfactory epithelium	Bis(chloromethyl) ether	Rat	Inhalation	(*22*)
Other regions of the nose					
Necrosis	Steno's glands	NNK	Rat	IP or SC (*20*)	

[a]Increased incidence in treated animals but probably spontaneous (see reference).

[b]Abbreviations: NNK, tobacco specific nitrosamine, 4-(*N*-methyl-*N*-nitrosamino)-1-(3-pyridyl)-1-butanone; IP, intraperitoneal injection; SC, subcutaneous.

respiratory tract the reader is referred to articles by Aharonson (*23*) and Morgan and Frank (*24*).

Uptake Studies

For the majority of these experiments, gas-laden air is passed through the upper airways of surgically prepared animals, using unidirectional flow systems. The gas concentrations entering and leaving the nose are used to determine the uptake efficiency. Other, less invasive approaches have also been devised for uptake studies in laboratory animals and humans (*25–40*). Table 2 lists findings derived from the majority of uptake studies reported to date. The nose removes a number of chemicals from inspired air, with uptake efficiencies ranging from almost 100% for formaldehyde in the dog (*33*) and hydrogen fluoride in the rat (*25*), down to less than 1% for carbon monoxide in humans (*40*) and dogs (*32*), with the other gases lying between these two extremes.

Examination of Table 2 reveals a good correlation between laboratory animals and humans for nasal uptake efficiency of sulfur dioxide, ammonia, and carbon monoxide, and a poorer correlation for acetone, the only other material for which data were available in humans and animals. It should be born in mind that many of these studies were carried out using widely different experimental procedures.

For details of studies that have used rats to investigate factors that influence nasal uptake of vapors by the nose, the reader is recommended to read the articles by Stott and McKenna (*26*), Morris et al. (*31*), and Morris and Cavanagh (*28,41*). These workers have investigated the relationship between gas uptake and water solubility, water/air and blood/air partitioning, airflow rate, species differences, nasal metabolism, and other factors. Stott et al. (*42*) have also described several pharmacokinetic models that may help in identifying physicochemical and physiological factors that influence uptake of chemical vapors by the upper respiratory tract.

Table 2. Uptake of selected gases and vapors by the nose or upper airways.

Gas or vapor	Species	Uptake efficiency, %[a]	Reference
Hydrogen fluoride	Rat	100	(*25*)
PGME	Rat	96	(*26*)
PGME acetate	Rat	94	(*26*)
Formaldehyde	Rat	93	(*27*)
Ethyl acrylate	Rat	66	(*26*)
Nitroethane	Rat	65	(*26*)
Epichlorohydrin	Rat	61	(*26*)
Styrene	Rat	57	(*26*)
Ethylene dibromide	Rat	49	(*26*)
Methylene chloride	Rat	13	(*26*)
Ethanol	Rat	32–84	(*28*)
Acetone	Rat	12–45	(*28*)
Sulfur dioxide	Rabbit	95–98	(*29*)
Ozone	Rabbit	50	(*30*)
Ozone	Guinea pig	50	(*30*)
Ethanol	Guinea pig	28–62	(*31*)
Acetone	Guinea pig	7–20	(*31*)
Ozone	Dog	100	(*32*)
Sulfur dioxide	Dog	100	(*32*)
Formaldehyde	Dog	99	(*33*)
Sulfur dioxide	Dog	95–97	(*34*)
Nitrogen dioxide	Dog	90	(*32*)
Ammonia	Dog	88–89	(*35*)
Ozone	Dog	80–87	(*36*)
Acrolein	Dog	78–80	(*33*)
Nitric oxide	Dog	73	(*32*)
Propionaldehyde	Dog	55–65	(*33*)
Acetone	Dog	52–60	(*35*)
Acetaldehyde	Dog	50–54	(*37*)
Carbon monoxide	Dog	0	(*32*)
Sulfur dioxide	Human	100	(*38*)
Ammonia	Human	83	(*39*)
Alcohol	Human	48	(*39*)
Hydrogen cyanide	Human	22	(*39*)
Acetone	Human	18	(*39*)
Carbon monoxide	Human	0	(*40*)

[a]Rounded to two significant figures.

Regional Deposition Studies

Very few attempts have been made to characterize regional deposition of inhaled materials in the nose. Whole body autoradiography demonstrated nasal deposition of ^{14}C derived from radiolabeled formaldehyde (*43*). However, attempts to use this approach to localize regional deposition patterns are confounded by the labile nature of reactive materials such as formaldehyde, which are rapidly metabolized or translocated from the deposition site. We could find no other experimental data on regional deposition of gases or vapors in the nasal passages of the rat.

Schreider (*44*) examined particle deposition in casts of guinea pigs and rats, using monodisperse aerosols of methylene blue, ranging in size from 1 to 7 μm in diameter. All the deposited material was found in the front third of the nose, with the highest concentration being just posterior to the nares. No material was found in the sinuses or smaller recesses. It was concluded that impaction, presumably as a consequence of nasal airflow patterns, was the principal process of deposition in the nasal passages for larger particles.

Torjussen (*45*) implicated airflow patterns in the deposition of particles on the anterior curvature of the middle turbinate of humans, and stated that this site-specific deposition probably accounts for the frequency of lesions in this site in nickel workers. Studies of particle deposition in the human nose using a radioaerosol revealed two major deposition sites that were correlated with airflow characteristics: close to the ostium internum where turbulent eddies are well developed, and the anterior region of the middle turbinate where the direction of airflow changes from upward to horizontal (*46*). These findings are consistent with the proposal made by Proetz (*47*) that airflow patterns play an important role in the regional deposition of inhaled materials in the nose, with the consequent potential to influence lesion location and severity.

Studies of Nasal Airflow

Species-specific differences in nasal airflow may be an important variable to consider during the process of determining human risk estimates using data derived from inhalation toxicology studies in rats. Studies of formaldehyde-toxicity in rats (*4,13,48*; Monticello et al., unpublished observations) and monkeys (*5*) demonstrated clear differences in the site specificity of lesions in the respiratory tract of these two species. The nasal passages of certain nonhuman primates, including rhesus (*49*) and cynomologous (Morgan et al., unpublished observations) monkeys provide a close anatomical model for the human nose. We therefore carried out studies of nasal airflow in rats and monkeys to determine the relationship between interspecies differences in nasal airflow patterns and the distribution of formaldehyde-induced lesions.

Several techniques have been devised to study airflow, some having been applied directly to the nasal passages, while others used nasal molds or models. These techniques have included the use of transducers to determine pressure-flow relationships, thermistor probes and hot-wire anemometry for studies of linear velocity, and laser anemometry for mapping of velocity fields. These approaches provide valuable quantitative data on nasal airflow but are not applicable to the very small nasal airways of the rat. Furthermore, while these techniques are useful for determining airflow characteristics in specific sites, they are not suitable for the determining overall flow patterns in complex airways.

Another approach to the study of nasal airflow is to create images on movie-film of smoke-laden air, or dyes dissolved in water, passing through transparent nasal models. A water-dye system was applied to the study nasal airflow in the baboon (*50*), the rat (*51*), and the monkey (Morgan et al., unpublished observations), using airway casts and molds.

Preparation of Airway Casts and Molds

A cast is a positive or solid representation of the airway, while a mold prepared from the cast is a negative or hollow model of the airway. Casts are made of opaque materials including silicone rubber, wax, metals, or plastics. Silicone rubber permits close examination of casts due to its flexibility, but it is not suitable for molding procedures involving small complex airways because it cannot be removed from the mold. Cerralow 117, a low melting point metal alloy that produces high-quality casts of biological structures as small as 25 μm diameter (*52*), was used by Schreider (*53*) to prepare casts and molds of nasal passages of guinea pigs. Molds are generally made from casts using optically clear materials, such as acrylic plastic. The aim of these procedures is to produce a transparent replica of the nasal airway. It is evident that defective casts or molds will result in artifacts which may yield misleading data.

A number of workers have made nasal casts and molds. For technical details of the complex and time-consuming processes involved in the preparation of a high-quality product, the reader should consult the articles of Collins (*54*) and Schreider (*53*), for human and guinea pig nasal passages, respectively. If multiple copies of a single cast or mold are required, a sandwich mold technique may be applied (*50*). The latter procedure is suitable for the large nasal airways of primates; as yet if has not been applied to rodents.

For our studies of airflow in the nasal passages of rats, the procedure of Schreider (*53*) was adopted with several modifications (*51*). The procedures developed for the present studies, which yielded high-quality casts and molds with a minimum of artifacts, have been reported previously (*51*) and are presented diagrammatically in Figure 3. An example of a nasal cast from a rat is shown in Figure 4, along with a diagram of the major nasal structures present in the cast in Figure 5. Plastic molds of the nasal passages of a rat and a cynomologous monkey are shown in Figures 6 and 7, respectively.

Determination of Airflow Characteristics in Nasal Molds

A water-dye model, with flow rates adjusted using a Reynold's conversion (*55*), was used to predict nasal airflow patterns. The clear nasal molds were connected to a tap water supply using stainless steel fittings, with Teflon and polyethylene tubing. A septum was fitted in the water supply upstream to the cast for the introduction of dyes (aqueous methylene blue or basic fuchsin) or India ink, by injection with a hypodermic syringe and a steel needle. A glass and steel ball flow meter, calibrated against tap water and connected between the water supply and the mold, was used to regulate flow rate. The cast was placed on the viewing surface of a dissecting microscope, fitted with a Bolex 16 mm movie camera with a motor drive to give a constant frame speed of 32 frames per sec. Flow recordings for monkey nasal molds were carried out as described previously for the baboon (*50*), using a telephoto lens in place of the microscope. Images, recorded on high-speed color film, were examined and analyzed with an analytical projector in both real-time and frame-by-frame modes.

Airflow rates, estimated to lie in the physiologic range, were determined from the respiratory minute volume and the sinusoidal pattern of inspiratory and expiratory airflow; they included low, intermediate, and maximal inspiratory rates. Water flow rates, to mimic these airflow rates, were then determined using a Reynold's conversion factor. The Reynold's conversion simply adjusts for the differing dynamic viscosities of air and water at room temperature (*55*).

Airflow Characteristics Based on Water Flow in Nasal Molds

It was evident from examination of the movie recordings of water-dye flow in these molds that nasal

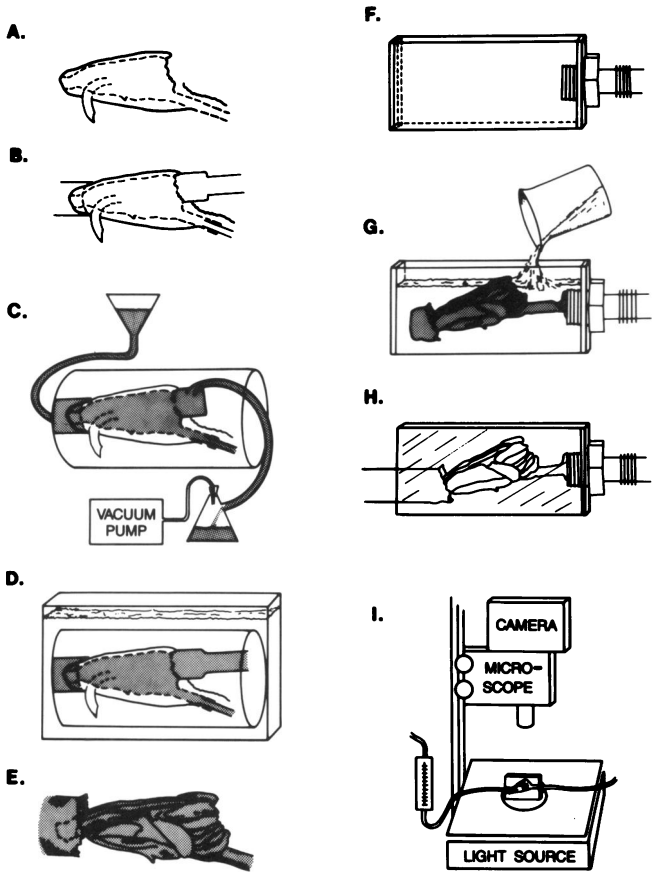

FIGURE 3. Diagram of casting and molding process for the nasal passages of rats. (A) Dissected head prepared for casting; (B) tubing attached; (C) head and tubing embedded in acrylic, and nasal passages are filled with casting metal from a funnel using a vacuum line; (D) epoxy and hot glue dissolved with methylene chloride and then tissues removed by soaking in potassium hydroxide; (E) metal cast after cleaning with water pick; (F) molding box prepared; (G) cast with fittings inserted in box which is then filled with clear molding plastic; (H) box detached from the outside of polymerized mold and metal cast removed from the inside using heat and dilute acid; (I) water-dye flow through the mold is recorded and analyzed using movie film.

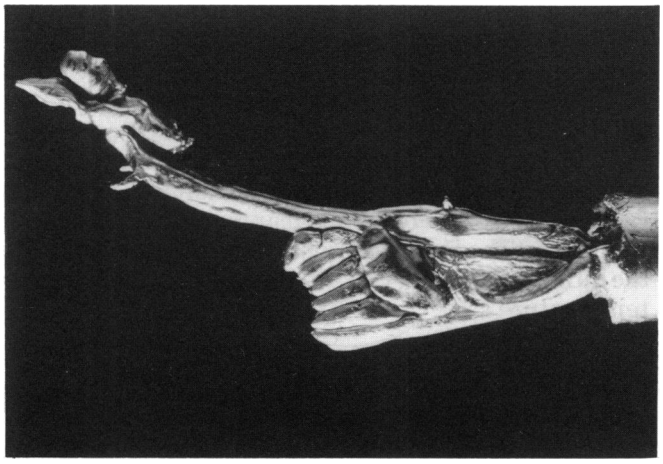

FIGURE 4. Metal cast of the nasal passages and larynx of a F-344 rat.

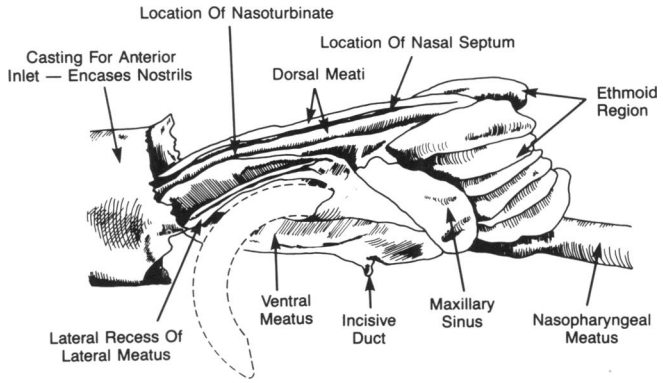

FIGURE 5. Diagram of cast of nasal passages indicating major structures.

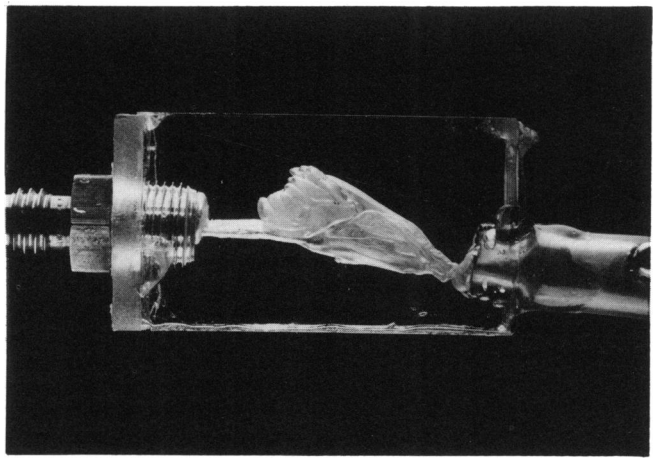

FIGURE 6. Clear acrylic mold of nasal passages of a F-344 rat.

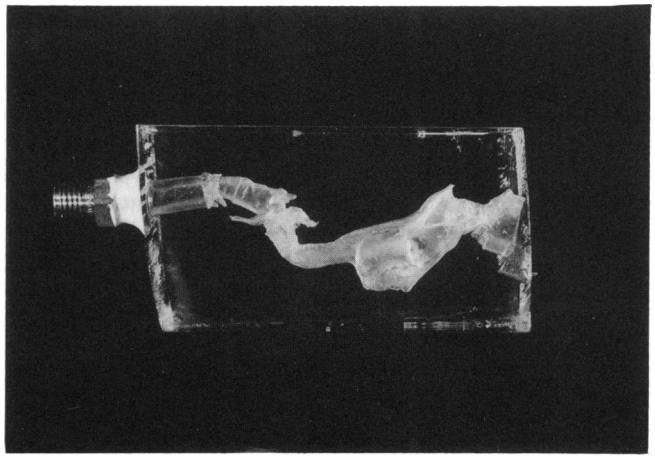

FIGURE 7. Clear acrylic mold of nasal passages of a cynomologous monkey.

airflow in rats and monkeys is extremely complex. Flow patterns were flow-rate dependent, and exhibited both bullet-shaped laminar flow and turbulent patterns with small and large vortices (whirlpoollike or circular flow). The major routes of flow during inspiration in the rat and monkey are presented in a simplified form in Figure 8.

In rats, the bulk of water flow in the anterior nasal passages passed along a region lateral to the nasoturbinate, referred to previously as the lateral meatus and lateral recess of the lateral meatus (*51*). The latter structure is apparently formed in close association with, and closely parallels, the dorsal surface of the roots of the incisor teeth (Figs. 4 and 5). In the monkey, the middle and ventral meati provided the major passageway for water flow. It is important to remember that these routes and patterns of flow were clearly rate dependent.

In the rat, higher rates of flow were associated with an increase in the amount of dye passing along the middle and dorsal meati with a characteristic narrow and very rapid stream of laminar flow in the middle meatus. Increased flow in the dorsal meatus would be expected to result in increased delivery of inhaled air to the olfactory mucosa. Characteristic vortices were observed in the anterio-dorsal aspect of the lateral meatus and at the anterior limit of the ventral meatus, again with clear flow rate dependency.

In the monkey, a prominent vortex occurred in the dorsal half of the nasal passages at higher rates of flow, which resulted in delivery of dye to the region of the nose that is lined by olfactory mucosa. Cynomologous monkeys, similarly to humans, have a large maxillary sinus that is connected to the middle meatus by a narrow ostium. There was no evidence of dye entering the maxillary sinus in these flow studies.

Many other complex flow patterns were observed, including a small but distinct oscillatory (almost wavelike) dorso-ventral displacement of all major streams at higher flow rates in the rat. This observation indicated interactions between different streams of water at higher flow rates that were not apparent at lower flow rates, presumably as a result of pressure-flow relationships throughout this complex system.

Correlation of Airflow Patterns with Lesion Distribution

In rats, the shape of the roots of the incisor teeth is reflected in the curved lateral recesses of the lateral meati of the anterior nasal passages. Examination of water-dye flow through molds in this region demonstrated that it was a major route of airflow during inspiration in the rat. There was also an apparent turbulence of this airstream as it passed from the narrow region of the nasal valve to the larger lateral meatus. Turbulence would be expected to enhance gas absorption by the nasal lining at all rates of airflow (*24*). Thus, the major airstream passing through the lateral meatus, and the associated regional turbulence, would lead to considerable direct exposure of the lateral aspect of the anterior half of the nasoturbinate and the adjacent lateral wall. The high water solubility of formaldehyde (55 g/100 mL) would also enhance uptake of this gas by the watery secretions lining this area of the nose. These proposals are consistent with the observations that acute lesions were most severe [(*13*); Monticello et al., unpublished observations], and nasal cancer most frequently originated (*4*) in the lateral meatus of rats exposed to airborne formaldehyde.

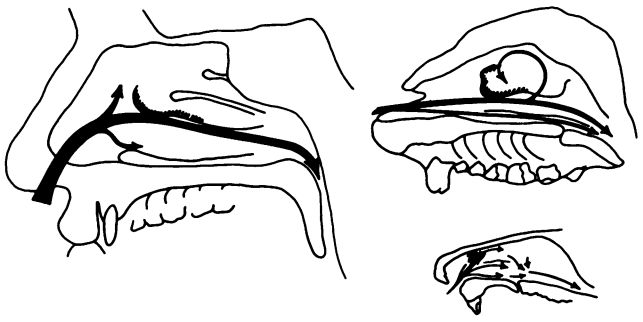

FIGURE 8. Simplified diagrams of nasal passages of man (left), cynomologous monkey (top right), and rat (lower right) drawn approximately to scale. Major routes of inspiratory airflow (arrows) in man were modified from Proetz (*47*) and Swift and Proctor (*55*). The common site for nasal lesions that have been associated with airflow patterns (see text) are indicated by cross-hatching. The major inspiratory route of flow in man and monkey is the middle meatus, passing close to the anterior curvature of the middle turbinate, while in the rat much of the air passes into the lateral meatus (see text for details).

In the human nose, most of the air flows along the middle meatus during inspiration (*55*), which probably accounts for the frequency of particle deposition and lesions on the anterior curvature of the middle turbinate in nickel workers (*45*) (Fig. 8). The nasal passages of rhesus and cynomologous monkeys anatomically resemble those of humans. In the present study the middle meatus was found to provide one of the major routes for inspired air in monkeys, indicating another similarity between monkeys and humans (Fig. 8). Responses to acute formaldehyde exposure in rhesus monkeys are most severe in regions adjacent to the major airstreams, especially on the ventral margin of the middle turbinate (*5*), indicating a correlation between airflow patterns and lesion distribution.

The absence of dye-flow into the maxillary sinus of the monkey was also consistent with studies of formaldehyde toxicity in monkeys, in which there was no evidence of histopathologic responses or changes in epithelial cell turnover rate following 1 or 6 weeks exposure to 6 ppm of formaldehyde (*5*). This observation provides further support for the conclusion of Monticello et al. (*5*), that combining tumors of the nasal cavity and sinuses in human epidemiologic studies is not appropriate for formaldehyde cancer risk assessment.

These studies demonstrated a good correlation between airflow patterns and the distribution of formalde-

hyde-induced lesions in rats and monkeys, with clear species differences with respect of airflow and lesion location. It is also noteworthy that the principal target site for formaldehyde in the nose of the rat (lateral meatus) is lined by a poorly ciliated cuboidal or low columnar epithelium with very few goblet cells. The major target site in the monkey (middle turbinate) is covered by densely ciliated columnar epithelium, with fairly numerous goblet cells. Thus airflow patterns may result in exposure of cell populations which differ, on the basis of morphologic and probably metabolic characteristics, between the rat and the monkey. These epithelia may also differ in their sensitivity to the carcinogenic properties of formaldehyde. Therefore, species differences in regional gas deposition as a result of nasal airflow characteristics may represent an important issue for consideration during human risk assessments based on studies in rats.

It was also interesting to note that increased inspiratory flow rates resulted in augmented delivery of dye to the olfactory region of the nose, the area which is responsible for the sense of smell. This observation is consistent with the role of sniffing, which results in higher inspiratory airflow rates. Such increases in airflow rate would be expected to contribute to olfactory activity by increasing exposure of the olfactory mucosa to air pollutants. However, in spite of producing a similar effect, the flow patterns responsible for the increased delivery of inspired air to the olfactory area differed markedly between the two species. Increased flow in the existing dorsal stream of the rat was replaced by a flow rate-dependent vortex (circular flow pattern) in the monkey. A similar vortex has been described as a feature of exhalation in human nasal passages (*47*).

It is important to remember that molds provide an imitation of the living nasal airway and have inherent limitations. The nose of live animals and people undergoes complex physiologic and structural changes, such as congestion of the nasal vasculature and movement of the nostrils (*56*). These changes cannot be mimicked by rigid airway models. Studies that are cognizant of these limitations should lead to valuable applications of nasal casts and molds.

Tissue Susceptibility

The nasal passages are lined by several different types of mucosa, each possessing characteristic morphologic (*51*), biochemical (*57–60*), and physiologic (*61*) properties that may influence their susceptibility to toxic chemicals. The olfactory epithelial toxicity of methyl bromide provides a good example of site-specific lesions that are probably a result of tissue susceptibility as a result of regional metabolism; they are unrelated to nasal airflow patterns (*18*). This gas is specifically toxic to olfactory epithelium, which is extensively destroyed in rats by a single 6-hr exposure to 200 ppm, while the other nasal epithelia remain morphologically unaffected. Methyl bromide has a very low water solubility (0.09 g/100mL), which results in slower uptake by the watery nasal secretions and thus greater access of this chemical to the recesses of the ethmoid region, resulting in a similar dose to all regions of the nose.

It has been proposed that the methyl bromide-induced degeneration of the olfactory epithelium in rats is the result of a primary biochemical lesion in olfactory sustentacular cells and mature sensory cells (*18*). Such a biochemical lesion would account for the site specificity of the epithelial damage seen at the light microscopic level.

Regional epithelial properties may also account for the distribution of responses in other areas of the nose. Histopathology has revealed that the squamous epithelial lining of the nasal vestibule is generally resistant to inhaled gaseous irritants (*2*), despite its exposed location. The transitional epithelium of the monkey, which lies between the squamous and respiratory epithelia in the nasal antrum, is specifically susceptible to ozone toxicity (*7*). The other major epithelial type in the nose, the respiratory epithelium, is a frequent site of lesions induced by inhaled gases or vapors in rats and monkeys. However, much of the respiratory epithelium lies in the major air passages and would be expected to receive higher exposure to inhaled air pollutants. Determining whether respiratory epithelial lesions are a consequence of specific sensitivity, or higher delivered dose to this region of the nose, is therefore problematic. We could find no good example of selective nasal respiratory epithelial toxicity in which the role of regional deposition could be ruled out.

Conclusions

The nose is a highly complex organ. It is evident that multiple factors may influence the distribution of lesions induced in the nose by inhaled gases or vapors. For highly water-soluble or reactive gases, such as formaldehyde, airflow patterns probably play a major role in regional deposition and consequent lesion distribution.

Studies on nasal airflow, described in this article, were carried out to assess further the value of the rat as a model for inhalation toxicology. This work has demonstrated clear differences in nasal airflow patterns between rats and primates. These differences should be considered when assessing data derived from rats for the purpose of assessing risks to humans from exposure to highly water-soluble or reactive gases such as formaldehyde. However, for poorly water-soluble gases such as methyl bromide, airflow appears to play only a minor role in lesion distribution, with regional tissue susceptibility being the major factor. For the majority of gases, which lie between the extremes of formaldehyde and methyl bromide with respect of water-solubility, the combined effects of airflow and tissue sensitivity will dictate the distribution and nature of nasal lesions.

The authors appreciate helpful comments and criticism from many collaborators, with special thanks to Jim Swenberg for introducing us to the field of nasal toxicology.

REFERENCES

1. Young, J. T. Histopathologic examination of the rat nasal cavity. Fund. Appl. Toxicol. 1: 309–312 (1981).
2. Jiang, X. Z., Morgan, K. T., and Beauchamp, R. W., Jr. Histopathology of acute and subacute nasal toxicity. In: Toxicology of the Nasal Passages (C. S. Barrow, Ed.), Hemisphere, New York, 1986, pp. 51–66.
3. Kerns, W. D., Pavkov, K. L., Donofrio, D. J., Gralla, E. J., and Swenberg, J. A. Carcinogenicity of formaldehyde in rats and mice after long-term inhalation exposure. Cancer Res. 43: 4382–4392 (1983).
4. Morgan, K. T., Jiang, X. A., Starr, T. B. and Kerns, W. D. More precise localization of nasal tumors associated with chronic exposure of F-344 rats to formaldehyde gas. Toxicol. Appl. Pharmacol. 82: 431–442 (1986).
5. Monticello, T. M., Morgan, K. T., Everitt, J. I., and Popp, J. A. Effects of formaldehyde gas on the respiratory tract of rhesus monkeys: pathology and cell proliferation. Am. J. Pathol. 134: 515–527 (1989).
6. Gross, E. A., Patterson, D. L., and Morgan, K. T. Effects of acute and chronic dimethylamine exposure on the nasal mucociliary apparatus of F-344 rats. Toxicol. Appl. Pharmacol. 90: 359–376 (1987).
7. Harkema, J. R., Plopper, C. G., Hyde, D. M., St. George, J. A., Wilson, D. W., and Dungworth, D. L. Response of the macaque nasal epithelium to ambient levels of ozone. A morphologic and morphometric study of the transitional and respiratory epithelium. Am. J. Pathol. 128: 29–44 (1987).
8. Giddens, W. E., Jr., and Fairchild, G. A. Effects of sulfur dioxide on the nasal mucosa of mice. Arch. Environ. Health 25: 166–173 (1972).
9. Jiang, X. Z., Buckley, L. A., and Morgan, K. T. Pathology of toxic responses to the RD50 concentration of chlorine gas in the nasal passages of rats and mice. Toxicol. Appl. Pharmacol. 71: 255–236 (1983).
10. Klonne, D. R., Ulrich, C. E., Riley, M. G., Hamm, T. E., Jr., Morgan, K. T., and Barrow, C. S. One-year inhalation toxicity study of chlorine in rhesus monkeys (Mucaca mulatta). Fundam. Appl. Toxicol. 9: 557–572 (1987).
11. Buckley, L. A., Jiang, X. Z., James, R. A., Morgan, K. T., and Barrow, C. S. Respiratory tract lesions induced by sensory irritants at the RD50 concentration. Toxicol. Appl. Pharmacol. 74: 417–429 (1983).
12. Reznik, G. Stinson, S. F., and Ward, J. M. Respiratory pathology in rats and mice after inhalation of 1,2-dibromo-3-chloropropane or 1,2-dibromoethane for 13 weeks. Arch. Toxicol. 46: 233–240 (1980).
13. Morgan, K. T., Gross, E. A., and Patterson, D. L. Responses of the nasal mucociliary apparatus of F-344 rats to formaldehyde gas. Toxicol. Appl. Pharmacol. 82: 1–13 (1986).
14. Lee, K. P., and Trochimowitz, H. J. Metaplastic changes of nasal respiratory epithelium in rats exposed to hexamethylphosphoramide (HMPA) by inhalation. Am J. Pathol. 196: 8–19 (1982).
15. Goldsworthy, T. L., Monticello, T. M., Jackh, R., Smith-Oliver, T., Bermudez, E., Morgan, K. T., and Butterworth, B. E. Assessment of 1,4-dioxane-induced carcinogenicity, genotoxicity and cell replication in rat nose and liver. Proc. Am. Assoc. Cancer Res. 29: 85 (1988).
16. Sellakumar, A. R., Snyder, C. A., and Albert, R. E. Inhalation carcinogenesis of various alkylating agents. JNCI 79: 285–289 (1987).
17. Torjussen, W., Solberg, L. A., and Hogetveit, A. C. Histopathological changes of the nasal mucosa in active and retired nickel workers. Br. J. Cancer 40: 568-580 (1979).
18. Hurtt, M. E., Thomas, D. A., Working, P. K., Monticello, T. M., and Morgan, K. T. Degeneration and regeneration of the olfactory epithelium following inhalation exposure to methyl bromide: pathology, cell kinetics, and olfactory function. Toxicol. Appl. Pharmacol. 94: 311–328 (1988).
19. Haschek, W. M., Morse, C. C., Boyd, M. R., Hakkinen, P. J., and Witschi, H. P. Pathology of acute inhalation exposure to 3-methylfuran in the rat and hamster. Exp. Mol. Pathol. 39: 342–354 (1983).
20. Belinsky, S. A., Walker, V. E., Maronpot, R. R., Swenberg, J. A., and Anderson, M. W. Molecular dosimetry and DNA adduct formation and cell toxicity in rat nasal mucosa following exposure to the tobacco specific nitrosamine 4-(N-methyl-N-nitrosamino)-1-(3-pyridyl)-1-butanone and their relationship to induction of neoplasia. Cancer Res. 47: 6058–6065 (1987).
21. Reznik-Schüller, H. M. Nitrosamine-induced nasal cavity carcinogenesis. In: Nasal Tumors in Animals and Man, Vol. 3 (G. Reznik and S. F. Stinson, Eds.), CRC Press, Boca Raton, FL, 1983, pp. 47–77.
22. Leong, B. K. J., Kochiba, R. J., and Jersey, G. C. A lifetime study of rat and mice exposed to vapors of bichloromethyl ether. TAP 58: 269–281 (1981).
23. Aharonson, E. F. Deposition and retention of inhaled gases and vapors. In: Air Pollution and the Lung (E. Aharonson, A. Ben-David, and M. A. Klingberg, Eds.), John Wiley and Sons, New York, 1976, pp. 13–24.
24. Morgan, M. S., and Frank, R. Uptake of pollutant gases by the respiratory system. In: Respiratory Defense Mechanisms (J. D. Brain, D. F. Proctor, and L. M. Reid, Eds.), Marcel Dekker, New York, 1977, pp. 157–189.
25. Morris, J. B., and Smith, F. A. Regional deposition and absorption of inhaled hydrogen fluoride in the rat. Toxicol. Appl. Pharmacol. 62: 81–89 (1982).
26. Stott, W. R., and McKenna, M. J. The comparative absorption and excretion of chemical vapors by the upper, lower and intact respiratory tract of rats. Fundam. Appl. Toxicol. 4: 594–602 (1984.)
27. Patterson, D. L., Gross, E. A., Bogdanffy, M. S., and Morgan, K. T. Retention of formaldehyde gas by the nasal passages of F-344 rats. Toxicologist 6: 55 (1986).
28. Morris, J. B., and Cavanagh, D. G. Deposition of ethanol and acetone vapors in the upper respiratory tract of the rat. Fundam. Appl. Toxicol. 6: 78–88 (1986).
29. Dalhamn, T., and Strandberg, L. Acute effects of sulphur dioxide on the rate of ciliary beat in the trachea of rabbit, *in vivo* and *in vitro*, with studies on the absorptional capacity of the nasal cavity. Int. J. Air Pollut. 4: 154–167 (1961).
30. Miller, F. J., McNeal, C. A., Kirtz, J. M., Gardner, D. E., Coffin, D. L., and Menzel, D. B. Nasopharyngeal removal of ozone in rabbits and guinea pigs. Toxicology 14: 273–281 (1979).
31. Morris, J. B., Clay, R. J., and Cavanagh, D. G. Species differences in upper respiratory tract deposition of acetone and ethanol vapors. Fundam. Appl. Toxicol. 7: 671–680 (1986).
32. Vaughan, T. R., Jennelle, L. F., and Lewis, T. R. Long-term exposure to low levels of air pollutants. Effects on pulmonary function in the beagle. Arch. Environ. Health 19: 45–50 (1969).
33. Egle, J. L. Retention of inhaled formaldehyde, propionaldehyde, and acrolein in the dog. Arch. Environ. Health 25: 119–124 (1972).
34. Brain, J. D. The uptake of inhaled gases by the nose. Ann. Otol. Rhinol. Laryngol. 79: 529–540 (1970).
35. Egle, J. L. Retention of inhaled acetone and ammonia in the dog. Am. Ind. Hyg. Assoc. J. 34: 533–539 (1973).
36. Yokoyama, E., and Frank, R. Respiratory uptake of ozone in dogs. Arch. Environ. Health 25: 132–138 (1972).
37. Egle, J. L. Retention of inhaled acetaldehyde in the dog. Arch. Environ. Health 24: 354–357 (1972).
38. Speizer, F. E., and Frank, N. R. The uptake and release of SO^2 by the human nose. Arch. Environ. Health 12: 725–728 (1966).
39. Landahl, H. D., and Herrmann, R. G. Retention of vapors and gases in the human nose and lung. Arch. Ind. Hyg. 1: 36–45 (1950).
40. Guyatt, A. R., Holmes, M. A., and Cumming, G. Can carbon monoxide by absorbed from the upper respiratory tract in man? Eur. J. Respir. Dis. 62: 383–390 (1981).
41. Morris, J. B., and Cavanagh, D. G. Metabolism and deposition of propanol and acetone vapors in the upper respiratory tract of the hamster. Fundam. Appl. Toxicol. 9: 34–40 (1987).
42. Stott, W. T., Ramsey, J. C., and McKenna, M. J. Absorption of chemical vapors by the upper respiratory tract of rats. In: Toxicology of the Nasal Passages (C. S. Barrow, Ed.), Hemisphere Publishing, New York, 1986, pp. 191–210.

43. Chang, J. C. F., Gross, E. A., Swenberg, J. A., and Barrow, C. S. Nasal cavity deposition, histopathology, and cell proliferation after single or repeated formaldehyde exposures in B6C3F1 mice and F-344 rats. Toxicol. Appl. Pharmacol. 68: 161–176 (1983).
44. Schreider, J. P. Nasal airway anatomy and inhalation deposition in experimental animals and people. In: Nasal Tumors in Animals and Man, Vol. 3 (G. Reznik and S. F. Stinson, Eds.), CRC Press, Boca Raton, FL, 1983, pp. 1–26.
45. Torjussen, W. Nasal cancer in nickel workers. Histopathological findings and nickel concentrations in the nasal mucosa of nickel workers, and a short review of chromium and arsenic. In: Nasal Tumors in Animals and Man, Vol. 2 (G. Reznik, and S. F. Stinson, Eds.), CRC Press Inc., Boca Raton, FL, 1983, pp. 33–53.
46. Itoh, H., Smaldone, G. C., Swift, D. L., and Wagner, H. N. Mechanisms of aerosol deposition in a nasal model. J. Aerosol Sci. 16: 529–534 (1985).
47. Proetz, A. W. Air currents in the upper respiratory tract and their clinical importance. Ann. Otol. Rhinol. Laryngol. 60: 439–467 (1951).
48. Morgan, K. T., Gross, E. A., and Patterson, D. L. Distribution, progression, and recovery of acute formaldehyde-induced inhibition of nasal mucociliary function in F-344 rats. Toxicol. Appl. Pharmacol. 86: 448–456 (1986).
49. Bridger, M. W., and van Nostsrand, A. W. The nose and paranasal sinuses—applied surgical anatomy. J. Otolaryngol. 7: (Suppl. 6) 1–33 (1978).
50. Patra, A. L., Gooya, A., and Morgan, K. T. Airflow characteristics in a baboon nasal passage cast. J. Appl. Physiol. 61: 1959–1966 (1986).
51. Morgan, K. T., Monticello, T. M., Fleishman, A., and Patra, A. L. Preparation of rat nasal airway casts and their application to studies of nasal airflow. In: Proceedings of a Symposium on Lung Dosimetry, Extrapolation Modeling of Inhaled Particles and Gases. Duke University, Durham, NC, in press.
52. McClenahan, J. L., and Vogel, S. F. The use of fusible metal as a radiopaque contrast medium and in the preparation of anatomical castings. Am. J. Roentgenol. Rad. Ther. Nucl. Med. 68: 406–412 (1952).
53. Schreider, J. P. Lung anatomy and characteristics of aerosol retention of the guinea pig. Ph.D. Dissertation, Department of Pharmacology and Physiological Sciences, The University of Chicago, Chicago, IL, 1977.
54. Collins, M. P. A practical guide to the construction of a *cire perdue* model of the human nose. Rhinology 23: 71–78 (1985).
55. Swift, D. L., and Proctor, D. F. Access of air to the respiratory tract. In: Respiratory Defense Mechanisms (J. D. Brain, D. F. Proctor, and L. M. Reid, Eds.), Marcel Dekker, New York, 1977, pp. 63–93.
56. Negus, A. The comparative anatomy and physiology of the nose and paranasal sinuses. Livingstone, Edinburgh and London.
57. Dahl, A. R., Hadley, W. M., Hahn, F. F., Benson, J. M., and McClellan, R. O. Cytochrome P-450-dependent monooxygenases in olfactory epithelium of dogs: possible role in tumorigenicity. Science 216: 57–59 (1982).
58. Randall, H. W., Bogdanffy, M. S., and Morgan, K. T. Enzyme histochemistry of the rat nasal mucosa embedded in cold glycol methacrylate. Am. J. Anat. 179: 10–17 (1987).
59. Bond, J. A., Harkema, J. R., and Russell, V. I. Regional distribution of xenobiotic metabolizing enzymes in respiratory airways of dogs. Drug Metab. Disp. 16: 116–124 (1988).
60. Baron, J. Burke, J. P., Guengerich, F. P., Jakoby, W. B., and Voigt, J. M. Sites for xenobiotic activation and detoxication within the respiratory tract: implications for chemically induced toxicity. Toxicol. Appl. Pharmacol. 93: 493–505 (1988).
61. Proctor, D. F., and Chang, J. C. F. Comparative anatomy and physiology of the nasal cavity. In: Nasal Tumors in Animals and Man, Vol. 1 (G. Reznik, and S. F. Stinson, Eds.), CRC Press, Boca Raton, FL, 1983, pp. 1233.